Numerical Evaluation of Non-homogeneity and Anisotropy due to Joints in Rock Media

S.A.Sadrnejad
Prof. Civil Eng. Dept., K.N.Toosi University of Technology, Teheran, Iran
Chancellor of Shahid Rajaii University, Teheran, Iran
E-mail:sadrnejad@hotmail.com, sadrnejad@srttu.edu

Abstract:An important concern in rock mechanics is non-homogeneity as joints or fault. Adopting the joints as fractures, fractures are well known for their effects on the mechanical and transport properties of rock.
It has been postulated that through fractured/jointed rock, mainly, the polygons turned to the shear vector (τ_i) are involved in the mobilization of shear resistance. Consequently, in order to locate the contact areas implicated into the shear-test it was firstly necessary to fix the shear direction. Moreover, since laboratory observations clearly show that only the steepest polygon surfaces touch the other sample, the identification of the potential sliding areas only requires the determination of the polygons which are faced to the shear direction and which, among them, are steep enough to be involved.
The methodology to be discussed here is modeling of slip on the local and global levels due to the distribution of deformation procedure of the rock joint. Upon the presented methodology, more attention has been given to slip initiation and propagation through rock joint. In particular, softening in non-linear behaviour of joint in going from the peak to residual strengths imparts a behaviour often associated with progressive failure.
A multi-plane based model is developed and used to compute plastic strain distribution and failure mechanism of rock joints. Validity of the presented model was examined by comparing numerical and test results showing the behavior of both homogeneous and jointed rock samples under general stress conditions.

Key words: anisotropy, jointed rock, multi-axial stress state, plasticity, hardening/softening law.

Introduction

A noticeable feature of rock media failures is the appearance of slip surfaces or shear band, the characteristics of that are associated with deformation being concentrated in narrow zones and the surrounding material remaining intact. The concept of a distinct failure plane that forms a wedge of material allows a direct examination of force equilibrium of the system and is central to most stability calculation (Hoek and Bray 1981). This problem includes a certain behavior of a local joint in global level due to the development of sliding and shear band. The softening observed in going from peak to residual strengths imparts a behavior often associated with progressive failure (Palmer and Rice 1973).

The multi-plane developed by Sadrnejad, (1992), is capable of predicting the behaviour of geo-materials such as rock on the basis of sliding mechanisms, elastic behaviour of intact parts and possibilities to see different plasticity models for the most possible sliding orientations. The induced/inherent anisotropy are included in a rational way without any additional hypotheses. According to the proposed model, the interface asperity shapes that are identical to model based on identifies the active sliding orientations, cracks, and joints. Furthermore, the sliding behavior of any predefined

[Downloaded from www.iust.ac.ir on 2024-10-03]

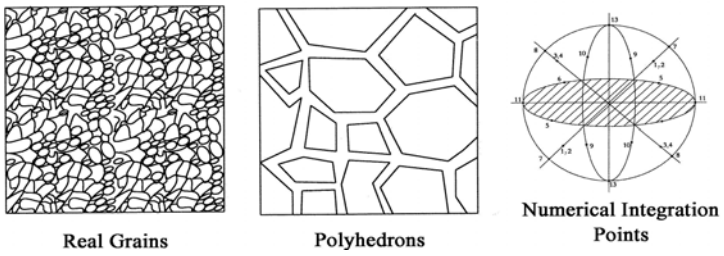

Fig.1-a Soil grains, artificial polyhedrons, sampling points

Direction Cosines			Weight	Direction cosins			Weight
ℓ_i	m_i	n_i	W_i	ℓ_i	m_i	n_i	W_i
$\sqrt{1/3}$	$\sqrt{1/3}$	$\sqrt{1/3}$	27/840	$\sqrt{1/3}$	$-\sqrt{1/3}$	$\sqrt{1/3}$	27/840
$-\sqrt{1/3}$	$\sqrt{1/3}$	$\sqrt{1/3}$	27/840	$-\sqrt{1/3}$	$-\sqrt{1/3}$	$\sqrt{1/3}$	27/840
$\sqrt{1/2}$	$\sqrt{1/2}$	0.0	32/840	$-\sqrt{1/2}$	$\sqrt{1/2}$	0.0	32/840
$\sqrt{1/2}$	0.0	$\sqrt{1/2}$	32/840	$-\sqrt{1/2}$	0.0	$\sqrt{1/2}$	32/840
0.0	$-\sqrt{1/2}$	$\sqrt{1/2}$	32/840	0.0	$+\sqrt{1/2}$	$\sqrt{1/2}$	32/840
1.0	0.0	0.0	40/840	0.0	1.0	0.0	40/840
0.0	0.0	1.0	40/840				

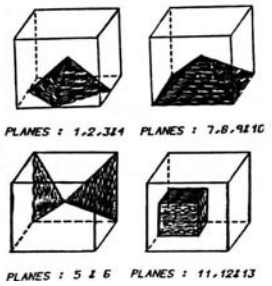

Fig.1-b Direction cosines, weighted coefficient, and Demonstration of 13 planes

existing joints through the rock mass is introduced to the matrix of global mechanical behavior based on a realistic and logical way.

Conceptual Discussion of Multi-plane frame work

Numerical integration generally simulates the smooth curved sphere surface to a composition of flat tangential planes make an approximated polygon to sphere surface. Any higher number of sampling planes, the approximated surface is more closed to sphere.

Rocks as other geo-materials support the overall applied loads through cohesion and contact friction; the overall mechanical response ideally may be described on the basis of micro-mechanical behaviour of intact parts interconnections. Multi-plane framework by defining the small continuum structural units as an assemblage of particles and voids that fill infinite spaces between the sampling planes, has appropriately justified the contribution of interconnection forces in overall macro-mechanics (Figure 1-a).

These assumptions adopt overall sliding, separation/closing of interaction of assumed intact parts included in one structural unit are summed up and contributed as the result of sliding, separation/closing surrounding boundary planes (Figure 1-b). This simply implies individual yielding/failure or even ill conditioning and bifurcation response or softening to be possible over any of the randomly oriented sampling planes.

Sliding Cracks

The condition of a sliding crack under compression is similar to the condition of shear bands. Accordingly, if such condition takes place at a point through continuum,

[Downloaded from www.iust.ac.ir on 2024-10-03]

the material stiffness is equal to a certain frictional resistance in the plane of sliding and normal material stiffness support the point along perpendicular direction with direction cosines of *{l,m,n}* . The sub-matrix stiffness of this point is calculated based on residual values of C'_r and φ_r. The reduction rule of these parameters is discussed later.

In the case of sliding crack under tension, the friction assumed to be reduced in such a way as free sliding condition is provided. The material sub-matrix stiffness at such a plane *{l,m,n}* supposed to be reduced by (3×3) sub-matrix (2). The penalty terms for this ideal condition come from the equation of where, means external multiplication sign. This requires that the following terms be added to the stiffness matrix:

$$\begin{bmatrix} (k_{3i-2,3i-2})(1-\ell^2) & -(k_{3i-2,3i-1})\ell m & -(k_{3i-2,3i})\ell n \\ -(k_{3i-1,3i-2})m\ell & (k_{3i-1,3i-1})(1-m^2) & -(k_{3i-1,3i})mn \\ -(k_{3i,3i-2})n\ell & -(k_{3i,3i-1})nm & (k_{3i,3i})(1-n^2) \end{bmatrix} \quad (1)$$

Tensile Cracks

While a typical point in concrete medium interferes crack upon either tensile stress/strain, it may be assumed that a planar lamination created that material strength may be negligible in normal direction to it. This orientation that conforms to one of the predefined sampling planes is identified as *{l,m,n}* . However, the strength of material in both of the plane of crack and normal to that are to change. While this point is allowed to move freely along a line with direction cosine *{l,m,n}*, the penalty term comes from setting $\delta_i .t = 0$, where, (δ_i) meaning is internal multiplication and *t* stands for orientation *{l,m,n}* . The existing stiffness at a typical point *i* before and after cracking are known as the following sub-matrices:

$$K_i = \begin{bmatrix} k_{3i-2,3i-2} & k_{3i-2,3i-1} & k_{3i-2,3i} \\ k_{3i-1,3i-2} & k_{3i-1,3i-1} & k_{3i-1,3i} \\ k_{3i,3i-2} & k_{3i,3i-1} & k_{3i,3i} \end{bmatrix} , \quad (2)$$

$$\begin{bmatrix} (k_{3i-2,3i-2})\ell^2 & (k_{3i-2,3i-1})\ell m & (k_{3i-2,3i})\ell n \\ (k_{3i-1,3i-2})m\ell & (k_{3i-1,3i-1})m^2 & (k_{3i-1,3i})mn \\ (k_{3i,3i-2})n\ell & (k_{3i,3i-1})nm & (k_{3i,3i})n^2 \end{bmatrix}$$

This condition is provided at a point through rock media, the ideal stiffness k_{ij} has been replaced by the real stiffness of material. This means that the point is free to move along *{l,m,n}* and the existing material stiffness is supporting the point to move on the plane perpendicular to *{l,m,n}* upon the proposed elasto-plasticity formulation.

The appropriate summation of all provided compliance matrices corresponding to considered slip planes yields overall C^p, therefore, strain increment at each stress increment is calculated as follows:

$$d\varepsilon^p = \frac{1}{n}\sum_{i=1}^{n} W_i [L_\varepsilon]^T C_i^p [L_\sigma] d\sigma' \quad (3)$$

L_ε and L_σ are transformation matrices for strain and stress, respectively and *n* is number of planes.

Constitutive Equations for a Sampling Plane

A sampling plane is defined as a boundary surface that is a contacting surface between two structural units of polyhedral blocks in

[Downloaded from www.iust.ac.ir on 2024-10-03]

rock media. These structural units are parts of an heterogeneous continuum and for simplicity they are defined as a full homogeneous and isotropic material. Therefore, all heterogeneities behaviour is supposed to appear in inelastic behaviour of corresponding slip planes.

Yield Criterion

In this constitutive formulation, the yield criterion is defined by the absolute ratio of shear stress (τ_I) to the normal effective stress (σ'_{ni}) on i^{th} sampling plane. The simplest form of yield function i.e. a straight line on τ versus σ_n space is adopted. As the ratio τ / σ_n increases, the yield surface represented by the straight line rotates anti-clock-wise due to hardening and approaches Mohr-Coulomb's failure line and finally failure on corresponding plane takes place.

The equation of yield function is formulated as follows:

$$F_i(\tau i, \sigma ni, \eta i) = \tau i - \sigma'_i - \eta_i \sigma_{ni} \qquad (4)$$

$\eta_i = tan(\alpha_i)$ is a hardening parameter and assumed as a hyperbolic function of plastic shear strain on the i^{th} plane. α_i is the slope of yield line and Ci is cohesion of soil.

To provide elastic behaviour of cohesion-less material whenever the direction of stress path changes, an elastic domain is considered. This domain as shown in Figure 2 is small and negligible. Therefore, the value of Φ_e for all type of grains in soils is assumed to be the same. However, to consider the cohesion of soil at the start of stress increment another elastic domain between the lines correspond to $\tau = \pm C$ has been defined. This domain also is shown in Figure 1. Consequently, the behavior of soil for $\tau < C_i$ is supposed to be elastic.

Plastic Potential Function

The plastic potential function is stated in terms of ti and si for the t - sn space as follows:

$$\psi(\tau_i, \sigma_{ni}) = \tau_i - C' + \eta_c . \sigma_{ni} . log_e(\sigma_{ni} / \sigma_{nic}) \qquad (5)$$

η_c is the slope of critical state line and snic is the value of effective normal stress the ith plane when $\tau_i = C'_i$. Typical presentations of this function are shown in Figure 2-a,b. The gradient of this function represents contractive and dilative behaviour in the ranges as:

$$0.0 \leqq \tau_i \leqq \sigma_{ni} . \eta_c \quad \text{(contractive behaviour)} \qquad (6)$$

$$\tau_i \geqq \sigma_{ni} . \eta_c \quad \text{(dilatant behaviour)} \qquad (7)$$

Derivative of this function is found as:

$$\partial \psi_i / \partial \sigma_i = \{1.0, \eta_c - \eta_i\}^T \qquad (8)$$

where, η_i is hardening parameter or the slope of yield line in i^{th} plane.

Obviously, dilatancy is positive if $\eta_i > \eta_c$ and negative if $\eta_i > \eta_c$ On critical state line $\eta_I = \eta_c$ and there is no volumetric plastic strain. For the soils predominantly composed of clay, a yield function the same as potential can be employed with associated the flow rule. In this case, a volumetric hardening rule besides shear hardening can present volumetric change during plasticity.

In theory of plastic flow, consistency condition is a necessary condition which requires that a yield criterion be satisfied as

[Downloaded from www.iust.ac.ir on 2024-10-03]

long as the material is in a plastic state. Mathematically, this condition is stated as follows:

$$\{\partial F_i/\partial\sigma\}^T.\mathrm{d}\sigma + \{\partial F_i/\partial K_i\}^T.\mathrm{d}K_i = 0.0 \quad (9)$$

where in the first loading process $K_i = \varepsilon^p{}_i$ and ε_i is plastic strain on the i^{th} plane. This relation can also be expressed in another form as:

$$d\varepsilon^p{}_i = \{1/Hp_i\}.\{\partial F_i/\partial\sigma_i\}^T.\{\partial\psi_i/\partial\sigma\}.d\sigma_i \quad (10)$$

where Hp_i is defined as hardening modulus of i plane and is obtained as follows:

$$Hpi = -\{\partial F_i \setminus \partial K_i\}^T . \{\partial\psi_i / \partial K_i\} \quad (11)$$

therefore,

$$d\varepsilon^p{}_i = C^p{}_i . d\sigma \quad (12)$$

where, $C^p{}_i$ is a 2×2 matrix and as a whole, represent the plastic resistance corresponds to the i_{th} active plane in plasticity and must be summed up as the contribution of this plane with the others after transforming into 6×6 size in global coordinate. Accordingly, the conceptual numerical integration of multi-plane framework presents the following summation for computing C_p.

$$C^p = 4\Pi.\sum_{i=1}^{n} W_i.L^T C_i^p L \quad (13)$$

where W_i are the weight coefficients and C_p is the global plastic compliance matrix corresponding to a single point in the medium and L is transformation matrix for the corresponding plane. n is the employed number of planes.

Hardening/Softening Rule

In this model an isotropic plastic shear hardening rule was employed for each plane. A simple function simulates the best variation of this property during the plastic flow which has been represented as a hyperbolic function as follows:

$$|\eta_i| = \frac{K_i.\tan(\phi_f)}{A_i + K_i} \quad (14)$$

where, $K_i = (\varepsilon^{pt}{}_i - \varepsilon^{pt}{}_{oi})$, Φ_f is peak internal frictional angle, and A_i is a soil parameter. $\varepsilon^{pt}{}_i$ and $\varepsilon^{pt}{}_{oi}$ are current and initial values of plastic shear strain on the i^{th} plane. It must be noted that at first loading $\varepsilon^{pt}{}_{oi}$ is equal to zero and its value is updated at each change of load increment sign. η_i starts from Φ_e, and grows accompanied with the plastic shear strain and slowly approaches the failure line. However, as stated for dense soils, it has to slowly rotate back towards the critical state line.

The strength reduction aspect as the changes of C_i and Φ_i adopted and the same elastic-plastic constitutive formulation is employed during softening sliding of planes. The reduction of parameters can be chosen as either of linear or exponential functions. Accordingly, C_i tends to a negligible value, while Φ_t tends to the residual friction Φ_r.

$$C_i = C_{i0}\ exp\ (-\zeta_n / \zeta_{si}) \quad (15)$$

$$\zeta_n = \zeta_{n-1} + d\zeta \quad (16)$$

$$\mathrm{d}\zeta = \tau_i.\mathrm{d}\varepsilon^{pt}{}_i \quad (17)$$

ζ_{si} is a softening parameter, C_{io} is initial cohesion and ζ_n is shear strain energy of i^{th} plane.

$$\Phi_I = arc\ tan\ [tan\ \Phi_r + (tan\ \Phi_o - tan\ \Phi_r)\ exp(-\zeta_n/\zeta_{st})] \quad (18)$$

[Downloaded from www.iust.ac.ir on 2024-10-03]

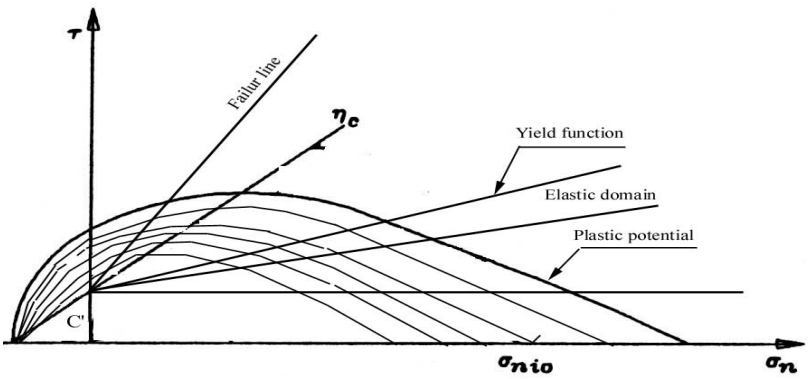

Figure 2 (a) functions in $\tau \sim \sigma_n$

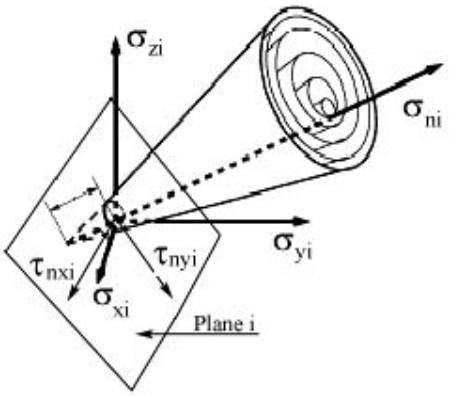

Figure 2 (b) yield function in 3D cordinate

Φ_I, Φ_r, and Φ_o are current, residual and initial friction angles respectively.

Any typical mechanical behavior of rock joints assumed to be elastic-plastic, with dilatancy, strain hardening/softening could be employed for planes. The strength reduction aspect as the changes of C_i and Φ_i adopted and the same elastic-plastic constitutive formulation is employed during softening sliding of planes.

To calibrate the model the mechanical results of two tests of one homogeneous rock sample and one including an identified joint are required. Assuming same parameters for all planes through homogeneous rock sample. Figures 3-a and 3-b show this calibration as the variation of axial load and volumetric strain versus axial strain. At the second stage, keeping all planes parameters the same and changing the plane parameters conformed to the joint in the sample, the calibration is done. In this way, the parameters for joint plane are obtained. Figures 3-c and 3-d show the results of second stage calibration for the case of having a 45^o inclined joint in the rock sample. In another case, the test results of the same rock sample including a 60^o inclined joint is considered and the joint plane parameters are carried out. Figures 3-e shows the result of this calibration. The main object

[Downloaded from www.iust.ac.ir on 2024-10-03]

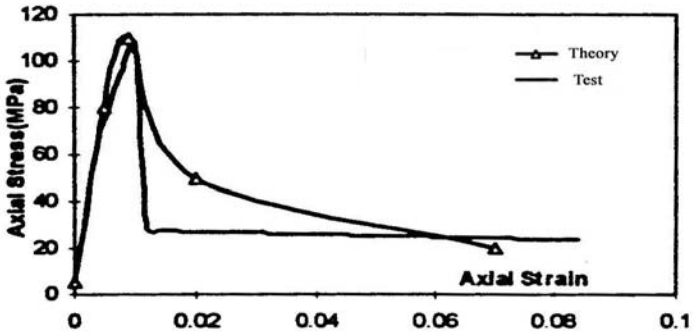

Figure 3-a Homogeneous rock sample

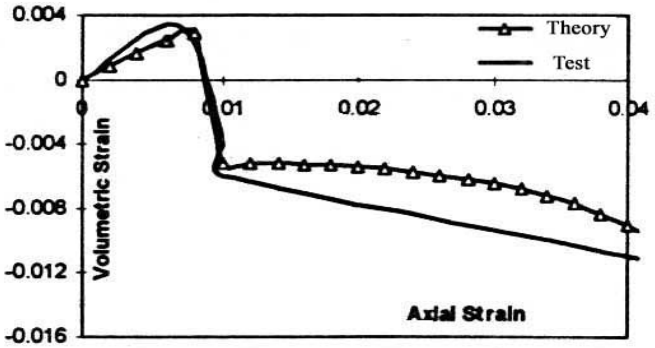

Figure 3-b Homogenious rock sample

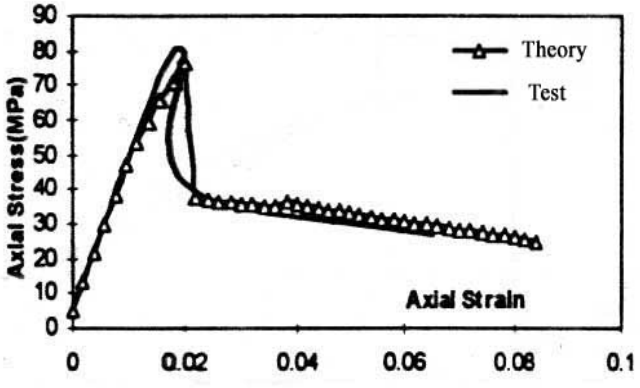

Figure 3-c Rock sample with 45^{o} inclined joint

[Downloaded from www.iust.ac.ir on 2024-10-03]

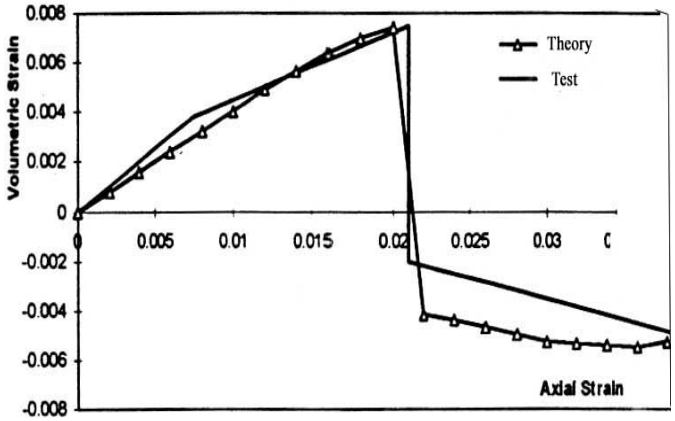

Figure 3-d Rock sample with 45^{o} inclined joint

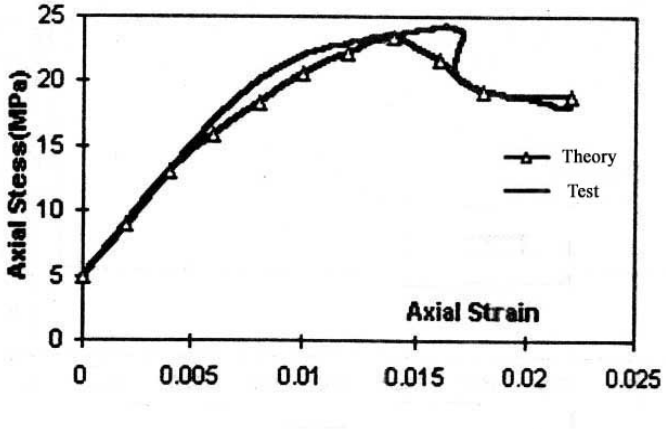

Figure 3-e Rock sample with 60^{o} inclined joint

Table 1 Parameter values

Parameter	Homogen rock	45° joint	60° joint
Elastic Modulus, E (Gpa.)	15	4	2
Poisson Ratio, ν	0.3	0.3	0.3
Critical State Line Slope, ηc	0.4	0.45	0.45
Hardening Parameter, Ao	0.0005	0.0005	0.0005
Friction Angle, φ*f*, (Degree)	35.52	35.52	35.52
Friction Angle, φ*f*, Plate No.1(60°)	35.52	35.52	17.65
Friction Angle, φ*f*, Plate No.7(45°)	35.52	27.21	35.52
Cohesion, Ci_0, (Mpa.)	10	4	4
Strain at start of Softening, (S)	0.0085	0.0085	0.0085
Softening parameters, ξ_{si}	0.7	0.75	0.78

[Downloaded from www.iust.ac.ir on 2024-10-03]

of this calibration is to find the effects of identified joint on the sample behavior.

Three set of parameters are carried out for homogeneous rock sample, sample including 45inclined joint and rock sample including a 60^o joint. These parameters are stated in Table 1.

Application of The Method

To Apply the presented method in an applicable boundary value problem, a two dimension rock surrounded tunnel is considered. The provided mesh, boundary conditions, and elements are shown in Figure 4-a. Three solutions are presented for the rock medium around the excavated tunnel. In the first solution rock medium is supposed to be made of homogeneous rock without any joint of non-homogeneity. The deformation contours at this conditions due to the excavation of tunnel is shown in Figure 4-b. Figures 4-c and 4-d show the obtained vertical and horizontal stress contours.

In the second and third solutions, it is assumed that the rock media to be made of rocks having joints inclined at 45^o and 60^o respectively. Different mechanical properties are employed for plane number 7 in second solution and plane number 1 in third solution as stated in table 1. Figures 5-a, 5-b, and 5-c are presented for the results of second solution and Figures 6-a, 6-b, and 6-c are for third solution.

To compare the three set of presented results, the maximum deformation of rocks at the peak point are compared. Table 2 shows the obtained values.

The variations of maximum displacement in vertical direction versus the assumed rock joint based on the three solutions are shown in Figure 7.

Conclusion

A powerful methodology based on a multi-plane elasto-plastic model is presented and successfully applied to show the capability of presenting the effects of any rock joint in mechanical behavior of rock structures. According to the presented method, the effects of an identified joint conforming to one of the pre-defined planes are seen in mechanical behavior through a simple calibration method.

Plastic behaviour of rock deposits in both intact and joint parts may possess different parameters and even stress-strain relationship. The possibility of introducing the features is presented in a multi-plane based model. Accordingly, the anisotropy of rock that is likely to be a decisive factor governing the plasticity response while the rock is even subject to principal stress rotation can be seen in the model.

The employed multi-plane based model can also been used for both intact and rock joint and is capable of predicting induced anisotropy, softening effects, pre-failure history of plastic strain distribution and failure orientation on plastic behaviour. This is fulfilled by distributing the effects of boundary condition changes into several predefined sampling orientations at one point and summing the micro-results up as the macro-result. The validity of the presented model was tested by comparing numerical and test results showing the behaviour of rock including any rock joint.
This framework is a development of constitutive models based on semi micro-mechanical aspects and theories of plasticity.

[Downloaded from www.iust.ac.ir on 2024-10-03]

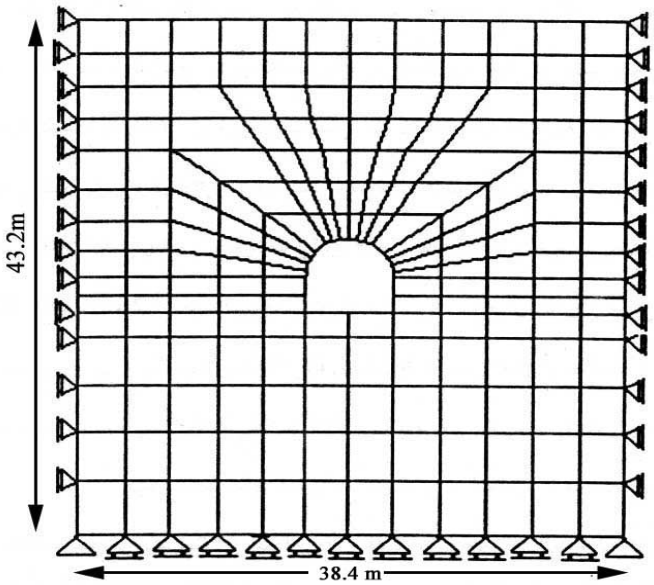

Figure 4-a Finite Element mesh for tunnel

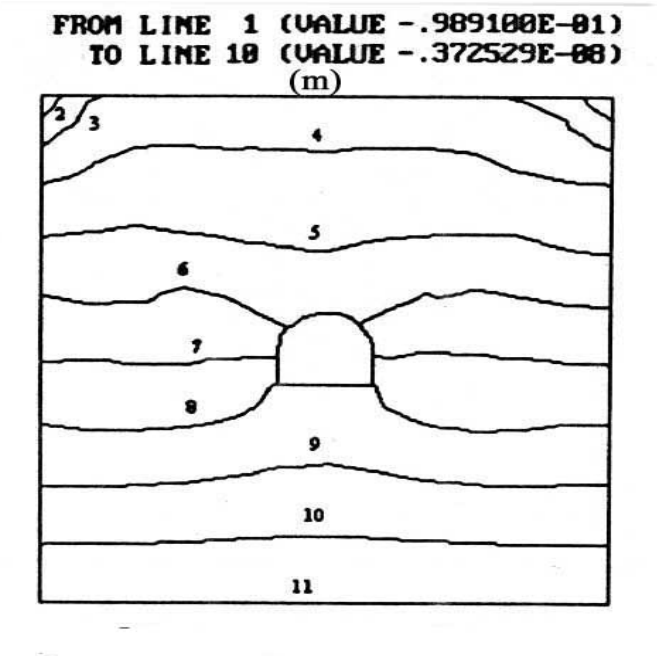

Figure 4-b Deformation of rock without joint

[Downloaded from www.iust.ac.ir on 2024-10-03]

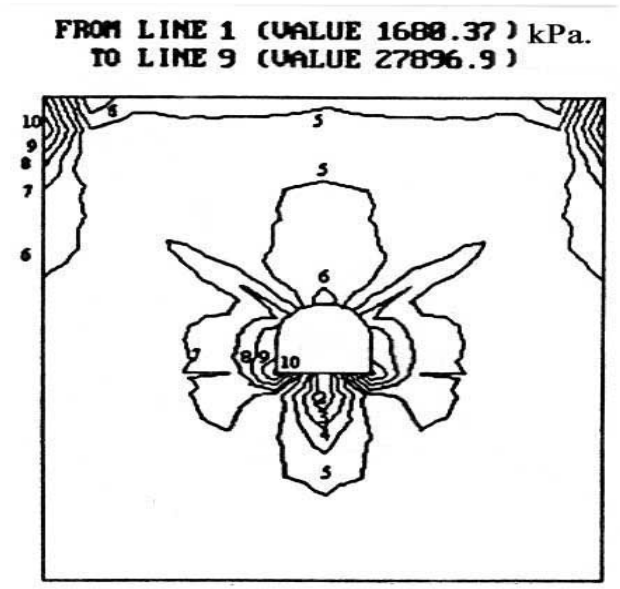

Figure 4-c σ_h in rock without joint

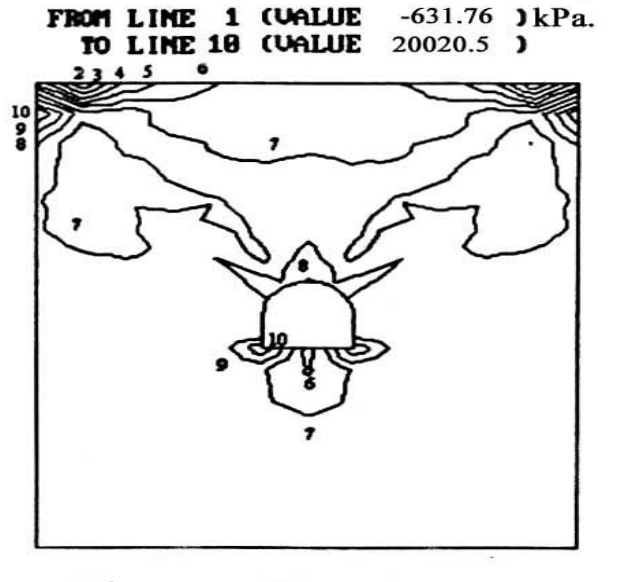

Figure 4-d σ_v in rock without joint

[Downloaded from www.iust.ac.ir on 2024-10-03]

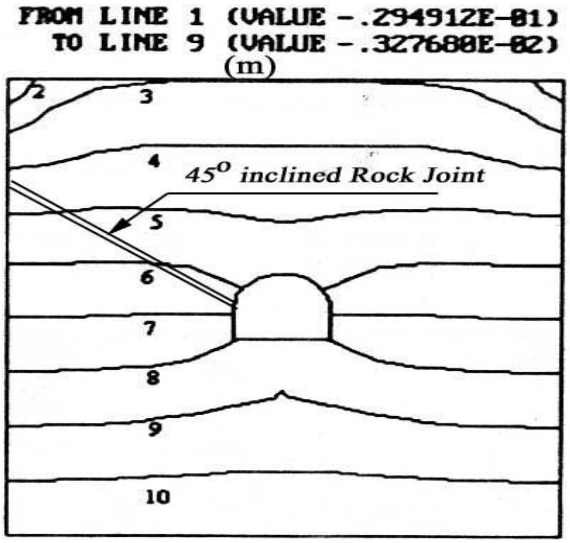

Figure 5-a Deformation of rock with 45º inclined joint

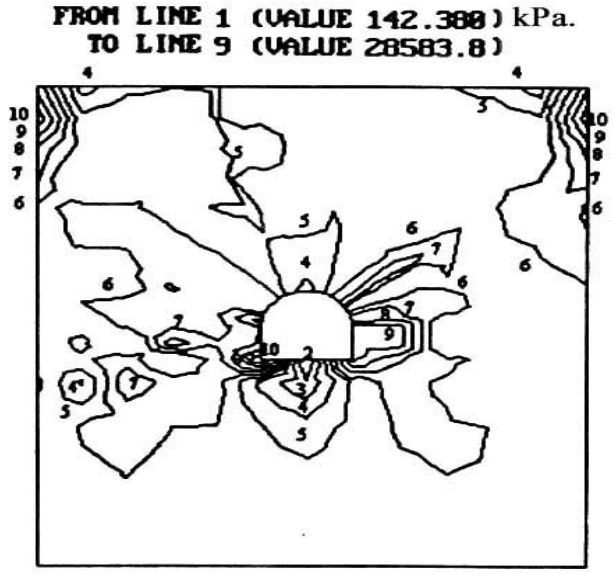

Figure 5-b σ_h in rock with 45º inclined joint

[Downloaded from www.iust.ac.ir on 2024-10-03]

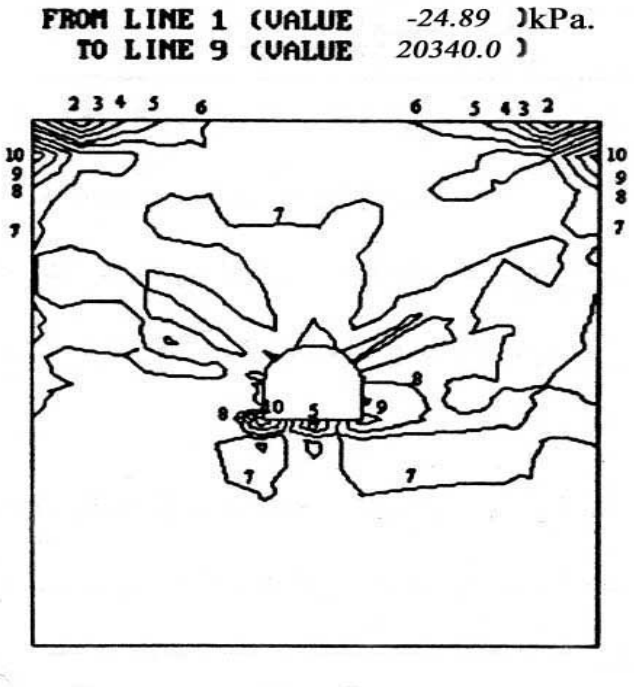

Figure 5-c σ_v in rock with 45° inclined joint

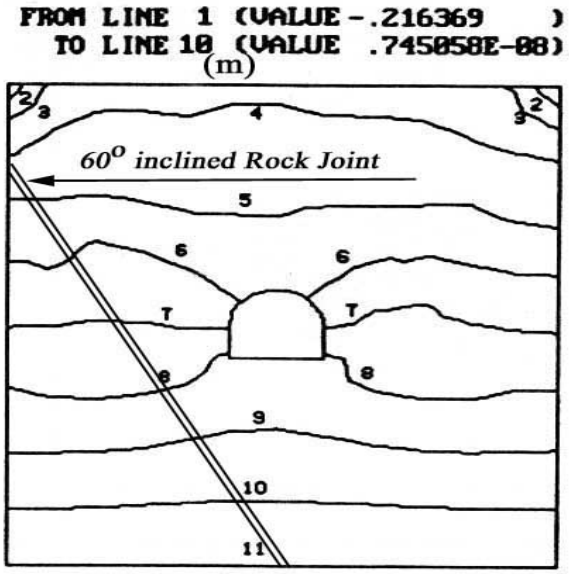

Figure 6-a Deformation of rock with 60° inclined joint

[Downloaded from www.iust.ac.ir on 2024-10-03]

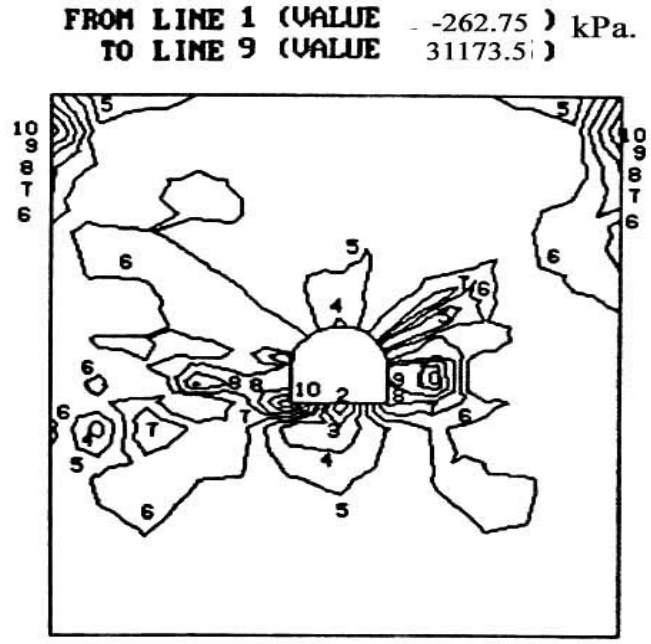

Figure 6-b σ_v in rock with 60° inclined joint

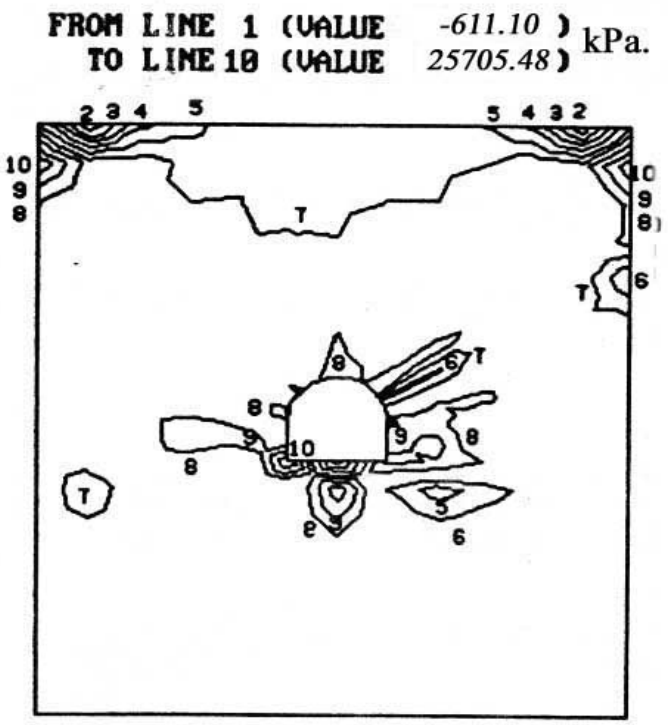

Figure 6-c σ_h in rock with 60° inclined joint

[Downloaded from www.iust.ac.ir on 2024-10-03]

Table 2 Maximum values of Deformation and Stress

Rock Condition	Def.(x) (cm)	Def.(y) (cm)	Stress(x) (kPa.)	Stress(y) (kPa.)
Homogeneous Rock	0.24	2..95	20020.5	27896.9
Rock with 45° joint	0.62	9.89	20340.0	28583.8
Rock with 60° joint	0.83	21.6	16785.8	38173.5

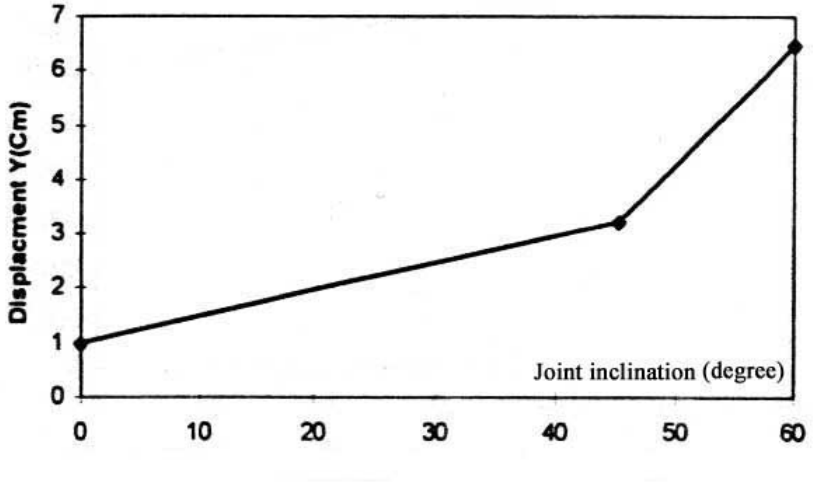

Figure 7 Maximum deformation versus joint inclination

[Downloaded from www.iust.ac.ir on 2024-10-03]

References

[1]. Abramowitz, M., and Stegun, I.A., (1965), "Handbook of Mathematical Functions", Dover Publications, inc., New York, 1965.

[2]. Aki, K. & Richards, P. G. (1980), Quantitative Seismology: Theory and Methods. W. H. Freeman and Company, San Francisco.

[3]. Barton, D.C., (1933), Surface fracture system of south Texas, Am Association Pet Geol Bull 17:1194-1212.

[4]. Cundall, P.A. & Hart, R.D., (1984), Analysis of block test No. 1 – Inelastic Rock Mass Behaviour; Phase 3 – A characterisation of joint behaviour (Final Report). Itasca Consulting Group Report, Rockwell Hand fords Operations, Subcontract SA-957 (cited from UDEC manual).

[5]. Hall, J., (1943), Geology of New York, Part 4. Survey of the forth Geological District. Albany, NY, 683 pp.

[6]. Hoek, E. & Bray, J. (1981), Rock Slope Engineering Institution of Mining and Metallurgy, London.

[7]. Palmer, C. A. & Rice, J.R. (1973), The growth of slip surfaces in the progressive failure of over-consolidation clay, Proceeding of Roy. Soc. London A, 332, 527-549.

[8]. Sadrnejad, S.A. (1992), 'Induced Anisotropy Prediction through Plasticity', Proceeding of International Conference on "Engineering Applications of Mechanics", June 9-12, 1992, Teheran-Iran, p.598-605.

[9]. Sadrnezhad S.A., (1992)," Multilaminate elastoplastic model for granular media", Journal of Engineering, Islamic Republic of Iran, vol.5, Nos.1&2, May, 1992

[Downloaded from www.iust.ac.ir on 2024-10-03]